Polymethine and squarylium molecules with large excited-state absorption

Jin Hong Lim [a], Olga V. Przhonska [a,1], Salah Khodja [a], Sidney Yang [a], T.S. Ross [a],
David J. Hagan [a], Eric W. Van Stryland [a,*], Mikhail V. Bondar [b],
Yuriy L. Slominsky [c]

[a] *School of Optics / CREOL (Center for Research and Education in Optics and Lasers), University of Central Florida, Orlando,
FL 32816-2700, USA*
[b] *Institute of Physics, National Academy of Sciences of Ukraine, Prospect Nauki 46, Kiev-22, 252650, Ukraine*
[c] *Institute of Organic Chemistry, National Academy of Sciences of Ukraine, Murmanskaya 5, Kiev-94, 253660, Ukraine*

Abstract

We study nonlinear absorption in a series of ten polymethine dyes and two squarylium dyes using Z-scan, pump-probe and optical limiting experiments. Both picosecond and nanosecond characterization were performed at 532 nm, while picosecond measurements were performed using an optical parametric oscillator (OPO) from 440 to 650 nm. The photophysical parameters of these dyes including cross sections and excited-state lifetimes are presented both in solution in ethanol and in an elastopolymeric material, polyurethane acrylate (PUA). We determine that the dominant nonlinearity in all these dyes is large excited-state absorption (ESA), i.e. reverse saturable absorption. For several of the dyes we measure a relatively large ground-state absorption cross section, σ_{01}, which effectively populates an excited state that possesses an extremely large ESA cross section, σ_{12}. The ratios of σ_{12}/σ_{01} are the largest we know of, up to 200 at 532 nm, and lead to very low thresholds for optical limiting. However, the lifetimes of the excited state are of the order of 1 ns in ethanol, which is increased to up to 3 ns in PUA. This lifetime is less than optimum for sensor protection applications for Q-switched inputs, and intersystem crossing times for these molecules are extremely long, so that triplet states are not populated. These parameters show a significant improvement over those of the first set of this class of dyes studied and indicate that further improvement of the photophysical parameters may be possible. From these measurements, correlations between molecular structure and nonlinear properties are made. We propose a five-level, all-singlet state model, which includes reorientation processes in the first excited state. This includes a *trans–cis* conformational change that leads to the formation of a new state with a new molecular configuration which is also absorbing but can undergo a light-induced degradation at high inputs. © 1999 Elsevier Science B.V. All rights reserved.

1. Introduction

Several classes of organic dye molecules show 'reverse saturable absorption' (RSA) in the visible

---

* Corresponding author. Fax: + 1-407-823-6880
[1] Permanent address: Institute of Physics, Prospect Nauki 46, Kiev-22, 252650, Ukraine.

spectral region. RSA leads to an increasing loss with increasing input and occurs when linear absorption creates excited states having absorption cross sections larger than that of the ground state. Typical ratios of excited to ground state absorption cross sections that show strong RSA are 10–20, while the ground-state absorption cross section is of the order of 10^{-18} cm^2 [1]. A significant ground-state absorp-

Table 1
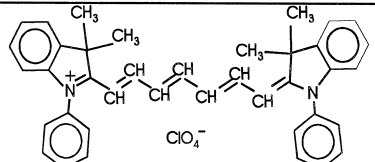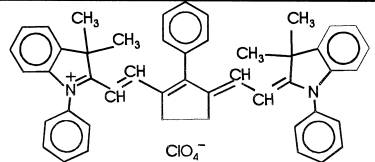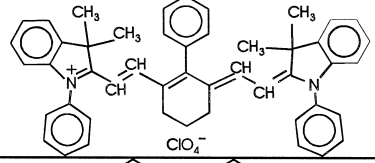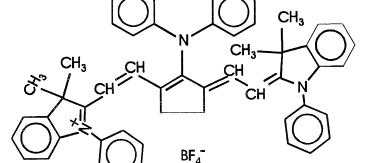Molecular structure of polymethine and squarilium dyes
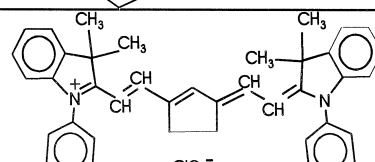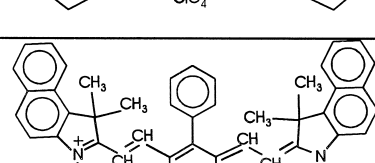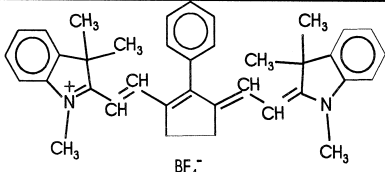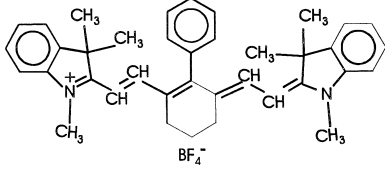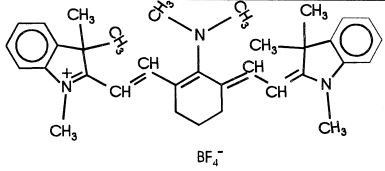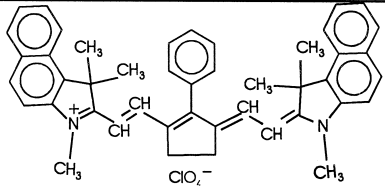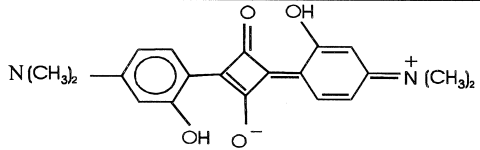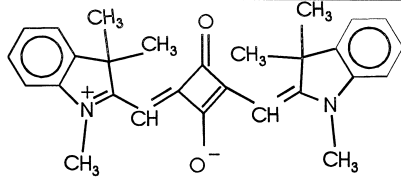
Dye	Molecular structure
PD1	
PD2	
PD3	
PD4	
PD5	
PD6	

Table 1 (continued)

Dye	Molecular structure
PD7	
PD8	
PD9	
PD10	
SD1	
SD2	

tion cross section is necessary to populate the excited state in the first place. Recently we reported RSA in several polymethine dyes (PD) in two host media (ethanol and the elastopolymer polyurethane acrylate, PUA) that showed considerably larger ratios while maintaining a similar ground state cross section [2]. One of these dyes showed a ratio of $\cong 80$ which is higher than previously reported ratios. This led to our current study, which is an investigation of the photophysical and nonlinear properties of a series of polymethine dyes with a systematic variation of their structure. We also present data for two other dyes of the squarylium class showing large RSA. We report the magnitudes of the absorption cross sections, lifetimes of the excited states and angular orientation data using polarized pump-probe experiments. In addition, we investigate the spectral dependence of one of PD and a squarylium dye in the visible from 440 to 650 nm.

One of the applications of RSA is for optical limiting devices that protect sensitive optical components including the human eye and other sensors from laser-induced damage [3,4]. Passive optical limiting has been demonstrated using RSA in a variety of organic and inorganic materials [5,6]. The best results were obtained in metallo-phthalocyanines and porphyrin dyes [7–10]. We contrast the current materials with metallo-phthalocyanine dyes indicating the larger RSA but also indicating problems for using PDs (and squarylium dyes) in optical limiting applications.

2. Materials

The molecular structures of the dyes studied are shown in Table 1 [2]. The room temperature linear absorption spectra are presented in Figs. 1 and 2 [3]. Spectroscopic properties of PDs are determined mainly by the existence of the delocalized π-electron system (polymethine chromophore or polymethine chain) with the transition dipole moment directed
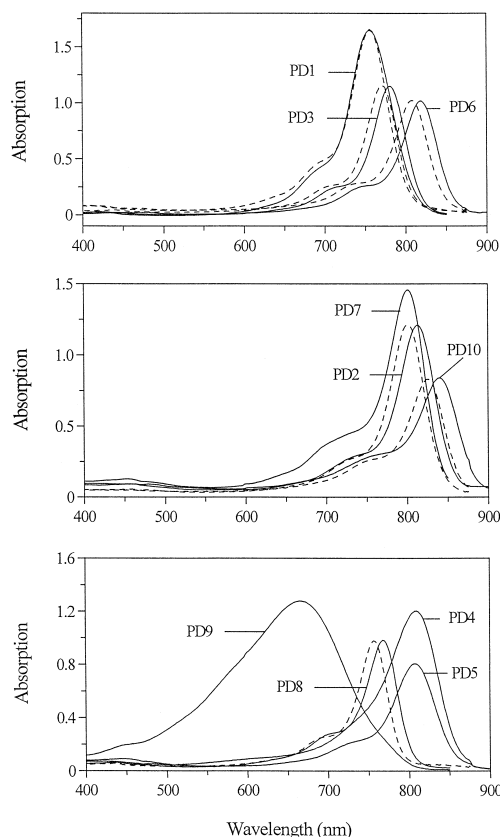
Fig. 1. Absorption spectra of PD1–PD10 in PUA (solid curves) and ethanol solutions (dashed curves).

along this chromophore. Changing the effective length of the polymethine chromophore (number of CH=CH groups) leads to a change in the position of the absorption band. The simplest way to shift the absorption maximum to the red region is to increase the number of CH=CH groups in the polymethine chain as demonstrated in Ref. [2]. In this case, a simple change of the number of CH=CH groups may drastically alter the limiting behavior. For example, a change from one group to two causes the nonlinear absorption to change from strong SA to strong RSA at 532 nm because the linear absorption peak is shifted out of resonance. A second way to shift the absorption spectrum to the red is to increase the effective length of the π-electron system at the end chromophore groups (so-called 'heavy' end groups) or to put a 'heavy' substitute into the polymethine chain. In this case, the interaction between

---

[2] Molecules synthesized at the Institute of Organic Chemistry, Kiev, Ukraine.

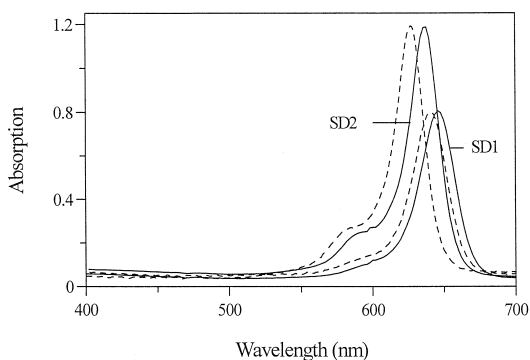[3] Data taken with a Perkin Elmer 330 UV–vis spectrophotometer.

Fig. 2. Absorption spectra of SD1–SD2 in PUA (solid curves) and ethanol solutions (dashed curves).

two conjugated π-electron systems (in the polymethine chain and end chromophore) leads to a lowering of the first excited state energy level. These effects can be seen from the data in Table 2. For example, PD1 with an unsubstituted polymethine chain has the shortest wavelength absorption resonance. (An exception is PD9 as explained below.) Inclusion of the 6-link cycle with a phenyl substitute in the polymethine chain (PD3) shifts the absorption peak to the red by 25 nm with respect to PD1. For PD6, the 6-link cycle red-shifts the peak by 62 nm. The difference lies in a more complicated π-electron system in the end chromophore groups for PD6.

A similar trend with change of chemical structure can be seen in the molecular series of dyes with a 5-link-cycle in the polymethine chain. Inclusion of a 5-link-cycle in the polymethine chain (PD5) shifts the absorption peak to the red region 51 nm (with respect to PD1) and by a similar amount for the dye with a 5-link-cycle and phenyl or biphenyl substitutes in the polymethine chain (PD2 and PD4). For PD10, with a more complicated π-electron system in the end chromophore groups, the red shift of the absorption maximum is the largest: compare PD1 (756 nm) with PD10 (840 nm). All comparisons are made for dyes in the PUA host. Thus, we are able to systematically modify the photophysical properties of the dyes, in particular, the frequency difference between the absorption resonance and the pumping laser frequency through changes in molecular structure.

The photophysical properties of PD9, distinguished structurally by a dimethylamino (DMA)-

substitution in the polymethine chain, are connected with the strong electron-donor ability of this group. Spectroscopic studies and quantum-chemical calculations for the analog of this dye [11] suggest that the blue shift in the absorption spectrum of almost 100 nm, with respect to PD8, is due to the strong donor properties of the DMA group. This leads to a decrease in the effective length of the π-conjugated system.

The two dyes at the end of Table 1 are squaraines or squarylium dyes: SD1 and SD2. Spectroscopic properties of SD1 are described in Ref. [12] and some nonlinear properties of SD2 are presented in Ref. [13]. The main distinguishing feature of squaraines is that their molecular structure consists of two electron-donor fragments connected with the central C_4O_2 acceptor group. Therefore, both the ground (S_0) and the first excited (S_1) states have an intramolecular charge-transfer character. They are characterized by large extinction coefficients and narrow absorption bands of the $S_0 \rightarrow S_1$ transitions. In the excited state, the internal rotation of the C–C linkages between the central C_4O_2 group and electron-donor end fragments can promote the nonradiative decay of this state. As will be described later for SD2, this rapid intramolecular twisting is the major reason for an observed quenching of the S_1 state in low viscosity solutions. In a rigid microenvironment surrounded, for example, by PUA, the squaraine molecules show a decreased rate of intramolecular twisting, leading to a significant increase in the fluorescence lifetime (more than ten times for SD2). It has been found that for SD1 the nonradiative excited-state decay may be inhibited by hydrogen bonding between the donor and acceptor parts of the dye molecule [12]. The presence of a hydroxyl group at the ortho position of each aromatic donor group leads to the formation of hydrogen bonds between these hydroxyl groups and the polar oxygen atoms of the central ring. This structure is rather rigid even in a low viscosity solution such as ethanol. Therefore, as will be experimentally shown later, a change in the surrounding environment from ethanol to PUA does not significantly influence the fluorescence lifetime.

All experiments were performed on these dyes in two host media: absolute ethanol and a PUA matrix. The polymeric guest–host matrices were obtained by

Table 2
Parameters of polymethine and squarylium dyes

Parameters	PD1 Ethanol	PD1 PUA	PD2 Ethanol	PD2 PUA	PD3 Ethanol	PD3 PUA	PD4 PUA	PD5 PUA	PD6 Ethanol	PD6 PUA	PD7 PUA	PD8 Ethanol	PD8 PUA	PD9 PUA	PD10 Ethanol	PD10 PUA	SD1 Ethanol	SD1 PUA	SD2 Ethanol	SD2 PUA
λ^{max} (abs) (nm)	755	756	800	812	770	781	810	807	807	818	801	757	768	666	826	840	640	647	627	637
Thickness (mm)	5.0	2.0	1.0	2.0	2.0	2.0	0.17	1.05	5.0	1.0	2.0	5.0	0.6	0.2	5.0	0.68	5.0	2.0	1.0	0.72
T_L	0.67	0.69	0.9	0.6	0.75	0.78	0.76	0.56	0.88	0.81	0.55	0.89	0.86	0.76	0.78	0.65	0.95	0.6	0.83	0.7
$\sigma_{0,1}$ ($\times 10^{18}$ cm^2)	4.5 ± 1.0	5.3 ± 0.7	9.0 ± 2.0	7.7 ± 1.0	1.5 ± 0.3	2.0 ± 0.3	17 ± 2	16 ± 2	1.8 ± 0.4	4.7 ± 1.0	17 ± 2	3 ± 1	5.3 ± 0.7	100 ± 15	7.0 ± 2.0	23 ± 3	24 ± 5	14 ± 2	22 ± 5	14 ± 2
σ_{12} ($\times 10^{16}$ cm^2)	5.5 ± 1.5	2.6 ± 0.5	0.5 ± 0.2	0.7 ± 0.2	3.0 ± 0.8	3.0 ± 0.6	1.8 ± 0.4	0.5 ± 0.1	2.2 ± 0.6	1.5 ± 0.3	0.6 ± 0.1	6 ± 1	2.7 ± 0.5	3.0 ± 0.5	1.4 ± 0.5	0.9 ± 0.2	2.0 ± 0.5	1.2 ± 0.2	4 ± 1	3.0 ± 0.5
σ_{12}/σ_{01}	120 ± 40	50 ± 10	6 ± 2	9 ± 2	200 ± 65	150 ± 30	11 ± 3	3.1 ± 0.7	120 ± 40	32 ± 7	3 ± 1	200 ± 60	50 ± 10	3.0 ± 0.5	20 ± 5	4 ± 1	8 ± 2	8 ± 2	18 ± 6	21 ± 5
τ_{S1} (ns)	1.1 ± 0.3	2.1 ± 0.5	1.0 ± 0.2	1.7 ± 0.4	1.0 ± 0.2	1.5 ± 0.2	1.5 ± 0.6	1.4 ± 0.3	0.5 ± 0.1	2.0 ± 0.2	1.4 ± 0.3	0.7 ± 0.2	2.2 ± 0.5	1.5 ± 0.4	0.5 ± 0.4	0.8 ± 0.2	6.0 ± 1.4	6.0 ± 1.4	0.4 ± 0.1	5 ± 1
τ_{S2} (ps)	0.2 ~ 0.3	2.9 ~ 3.9	1.5 ~ 1.9	1.5 ~ 2.3	1.8 ~ 2.0	1.8 ~ 2.0	0.5 ~ 0.8	1.0 ~ 1.7	1.0 ~ 1.3	0.7 ~ 1.2	1.4 ~ 1.9	2.1 ~ 2.7	2.3 ~ 2.9	1.5 ~ 2.0	0.4 ~ 0.6	0.7 ~ 1.0	0.2 ~ 0.4	0.5 ~ 1.0	1.7 ~ 2.3	1.8 ~ 2.7
τ_F (ns)	0.15	0.6	0.15	0.5	0.2	0.5	0.5	0.6	0.1	0.6	0.5	0.2	0.5	0.5	0.1	0.5	0.3	0.85	0.15	2.5

a previously reported radical photopolymerization procedure [14]. First, we prepared a liquid photosensitive mixture of oligourethane acrylate, dye and photoinitiator. This mixture, held between two glass or quartz plates, was irradiated at the absorption band of the photoinitiator, resulting in polymerization. The polymerization of oligomers is characterized by a small shrinkage, only about 2–3% of its original volume, which is significantly less than the shrinkage upon the polymerization of monomers. The dye molecules are not chemically bound, but are dissolved in the polymer matrix. The advantages of this method are that the dye molecules neither aggregate nor form a complex with the polymeric matrix. Therefore, their absorption characteristics do not change significantly from those previously determined in liquid media. With this technology, it is possible to incorporate many different classes of dyes into PUA.

The main feature of PUA is the existence of a highly elastic state at room temperature. The elastic properties of PUA described in Ref. [14], and the peculiarities of the radical photopolymerization procedure determine the construction of optical elements. The glass or quartz plates are necessary to contain the material during the polymerization procedure, establish high optical quality of the polymer layer and protect the optical element from mechanical damage and atmospheric exposure. Strong adhesion between the surface of the plates and the polymer layer is observed. Protection of the optical element from atmospheric oxygen is very important because photo-oxidation is one of the major mechanisms for photodegradation of organic dyes.

The thickness of the polymer layers varies from 0.1 to 2 mm in order to satisfy both linear (0.1–0.2 mm and 0.8–2 mm) and nonlinear (about 0.8–2 mm) absorption characteristics. The concentration of the dyes varies from 10^{-5} to 10^{-3} mol/l. The absorption spectra in PUA show a small red shift in comparison to the ethanol solutions. This shift is smallest for unsubstituted PD1 (1 nm) and largest for PD10 which has a 5-link-cycle and phenyl substitute in the polymethine chain (14 nm). The structure of the bands and their half-widths are similar in ethanol and in PUA. Special attention was given to the photopolymerization procedure in order to reduce the rate of photobleaching of the dyes and avoid the appearance of their photoproducts. It was shown in our previous article [2], that the appearance of photochemical products in PUA during the preparation of the samples led to a substantial increase in linear absorption at 532 nm. Choosing the proper initiator and its concentration minimized photodecomposition.

The concentration of the polymethine PD3 is 1.1×10^{-3} mol/l in PUA and 1.03×10^{-3} mol/l in ethanol, while that of the squarylium SD2 is 3.4×10^{-3} mol/l in PUA and 1.4×10^{-4} mol/l in ethanol. The corresponding sample thicknesses are: for PD3, 2 mm for PUA and 2 mm for ethanol; and for SD2, 0.65 mm for PUA and 2 mm for ethanol. These dyes were singled out for more intensive wavelength dependent studies due to their large RSA response at 532 nm.

3. Experimental methods

We used three well-developed nonlinear characterization techniques: Z-scan [15] (with both pico- and nanosecond pulses), optical limiting measurements, see for example [16] (for nanosecond laser pulses) and picosecond pump-probe experiments [17]. Many of the experiments were conducted at 532 nm using the second harmonic of Nd:YAG with both picosecond and nanosecond pulses, although Z-scans and pump-probe measurements were also performed on PD3 and SD2 at wavelengths from 450 nm to 650 nm using a picosecond optical parametric oscillator (OPO). For the picosecond 532 nm studies, we used an active/passive modelocked Nd:YAG laser and switch out a single pulse from the 40 ns long train of pulses each separated by 7 ns. This pulse was frequency doubled to give a single pulse of temporal width 30 ps (FWHM) at 532 nm and a repetition rate that could be adjusted from single shot up to 10 Hz. In some experiments, to determine the nanosecond response, the whole frequency doubled pulse train could be used. For nanosecond studies, we also used a Q-switched laser with a pulsewidth of 10 ns (FWHM) at 532 nm having a repetition rate of 10 Hz. The spatial beam profile from both laser systems was Gaussian.

The tunable source was a singly-resonant, picosecond OPO synchronously pumped by the third-

harmonic of the modelocked train of Nd:YAG pulses described above. The OPO was continuously tunable from 400 to 700 nm using two critically phase-matched BBO crystals mounted for walkoff compensation. This produced a train of pulses, from which single pulses could be selected using a voltage tunable Pockels cell. The linewidth of the pulse train was 0.5 nm to $\cong 1.5$ nm (HW1/eM), depending on wavelength. The single OPO pulses used had a pulsewidth of $\cong 14$ ps (FWHM) and energy of approximately 2 μJ. The OPO Z-scans reported here were all performed in the single pulse mode.

The Z-scans we performed are 'open aperture' where the total energy transmitted by the sample was measured as a function of the sample position Z with respect to the focal position of the input beam [15]. The incident energy was held constant during a Z-scan so that the irradiance and fluence (energy per unit area) varied with Z. The range of energies used was 0.01–70 μJ. For all 532 nm Z-scans, the beam was focused to a waist of radius 22 μm (HW1/e^{2}M) for picosecond pulses and 30 μm (HW1/e^{2}M) for nanosecond pulses. Similar sizes were used for the OPO Z-scan experiments. Care was taken to collect all the energy so that these open aperture Z-scans were sensitive only to nonlinear absorption.

Optical limiting curves were measured with 10 ns (FWHM), 10 Hz, 532 nm laser pulses, in which the samples were located at the focal position of the input beam, corresponding to the minimum transmittance as determined from Z-scan measurements. The pumping beam was focused to a waist of calculated radius 5 μm (HW1/e^{2}M, assuming a diffraction limited Gaussian beam). Each limiting curve was measured within two or three input energy regions. Continuous variation of the input energy was obtained by rotating a half-wave plate in front of a fixed polarizer.

Pump-probe experiments were used to study the dynamics of photoinduced absorption and determined excited-state lifetimes. In these measurements a strong pump beam changed the absorption of the sample which was probed at delay times up to 15 ns by a weak probe beam. Pump-probe measurements were performed for probe pulses polarized parallel and perpendicular to the pump pulse. At 532 nm the pump beam was focused to a waist of radius 230 μm (HW1/e^{2}M), while the probe beam was focused to

a waist of radius 34 μm (HW1/e^{2}M). The range of pumping energies was 10–150 μJ. The probe irradiance was kept much less than the pump irradiance so the probe beam did not induce any significant nonlinearity. Both pulses were recombined at a small angle ($\cong 5$ degrees) within the sample.

The pump-probe geometry used with the OPO source was similar except that, due to the reduced available energy, the spot sizes were reduced. The beam waists of the pump pulse were 86–94 μm (HW1/e^{2}M) depending on wavelength, and the beam waist of the probe pulse was ~ 40 μm. Pump energies were 0.9–1.4 μJ. The probe beam was delayed up to 6 ns and its energy was kept approximately 500 times lower than the pump energy. The two beams were focused at the same position inside the sample and the angle between the pump and probe beam was $\cong 4$ degrees.

4. Results

We analyze the following data in terms of one of the level structures shown in Fig. 3. Unless specifically noted, the results are interpreted in terms of the simple 3-level model of Fig. 3(a). However, as discussed below, this model is inadequate to explain all of the data, which requires the more elaborate 5-level model of Fig. 3(b).

4.1. Measurements at 532 nm

4.1.1. Picosecond Z-scans at 532 nm

We studied the nonlinear transmittance at 532 nm of PD1–PD10 and SD1–SD2 in ethanol solutions and in PUA over a wide range of input fluences from 0.0001 to 1 J/cm^2. All the samples (except PD9) exhibited RSA as 532 nm radiation produced excitation into the short wavelength tail of the linear absorption band. The values of the ground state absorption cross section, σ_{01}, were in the range of 1.5×10^{-18} to 2.4×10^{-17} cm^2, depending on dye molecular structure, except for PD9 which has $\sigma_{01} \cong 10^{-16}$ cm^2 since the broad absorption band was shifted enough to include 532 nm. These values are shown in Table 2.
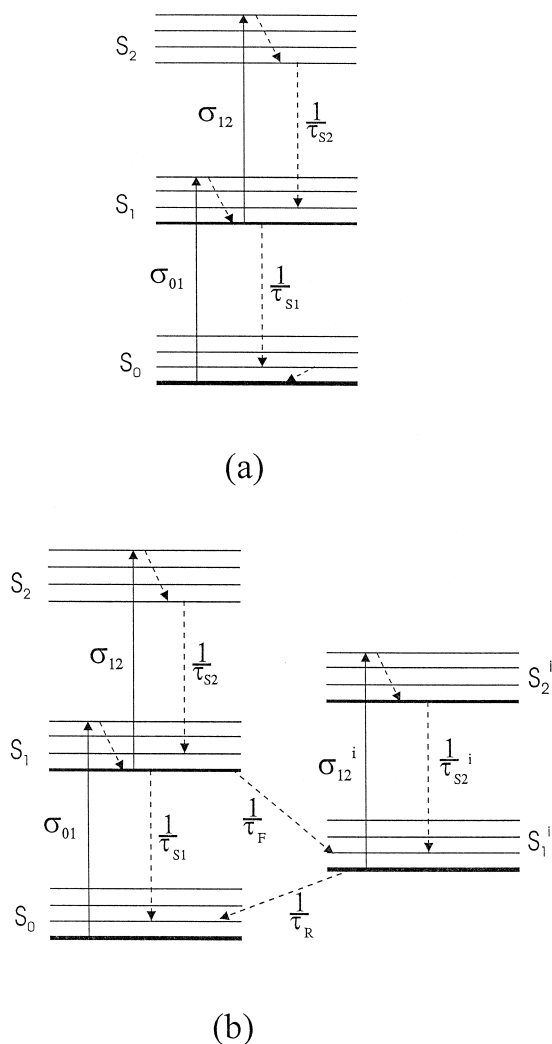
(a)

(b)

Fig. 3. (a) 3-level and (b) 5-level model for polymethine and squarylium dyes. S_0, S_1, S_2, S_1^i and S_2^i are singlet states. σ_{01}, σ_{12} and σ_{12}^i are absorption cross sections and $1/\tau_{S1}$, $1/\tau_{S2}$, $1/\tau_F$, $1/\tau_R$ are rate constants. The series of horizontal lines within each singlet state are vibrational energy levels.

With repeated irradiation at fluence levels greater than $\cong 0.3$–1 J/cm^2, depending on the dye and medium, (irradiances greater than $\cong 9$–30 GW/cm^2) we observed a marked permanent reduction of the nonlinear response for all the dyes which we refer to as photodegradation. Similar but unrelated effects have been observed by many authors, for example, Refs. [18–21], and explained by saturation

of the absorption of the $S_1 \rightarrow S_2$ transition of Fig. 3(a). While this type of saturation certainly affects the numerical fitting of data for picosecond inputs (the S_2 lifetime is determined from such fits), it is not the cause of the large reduction of nonlinear response at very high inputs, as explained below. In a previous paper, Ref. [2], we performed Z-scans at various repetition rates from 10 Hz to 0.5 Hz and also moved the sample between laser firings in order to irradiate a fresh site after each pulse. Increasing the time between pulses (or changing the spot at the sample) led to a decrease of this photodegradation in all the samples in either host. This can be explained by a photochemical decomposition into a new photoproduct with low absorption at 532 nm due to a laser-induced reaction occurring in the excited state. The slow recovery observed in the experiments was due to diffusion of fresh molecules into the focal volume. This was determined by irradiating different spot sizes and noting that the recovery time lengthened with increasing spot size. This occurred even in PUA, but at a much reduced rate as compared to ethanol (tens of minutes as opposed to seconds). A more detailed understanding of these processes requires additional investigation. In this paper we concentrated on studying the nonlinear absorption of the dyes at fluences below those that produce photodegradation. As explained later in this paper, this degradation appears to be initiated by a chemical reaction after a *trans–cis* conformational change in the excited state. *trans–cis* conformational changes, also revealed by the pump-probe experiments, are also suppressed by the polymeric host.

In Fig. 4, we show open-aperture picosecond Z-scans at 532 nm for one of the most nonlinear dyes, PD3 in PUA (Fig. 4(a)) and in ethanol (Fig. 4(c)) at fluences from 0.013 J/cm^2 to 4.2 J/cm^2. As can be seen in the picosecond regime, the transmittance was reduced by a factor of four at high fluence (linear transmittance is 78%, sample thickness 2 mm). At fluences > 0.3 J/cm^2 for PUA and > 0.7 J/cm^2 for ethanol, photodegradation was observed. If degradation of the sample occurs during the performance of an open-aperture Z-scan it will appear asymmetrical (scans are performed form the left to right in the figures). Molecular parameters are extracted for inputs lower than the values that produce photodegradation for all the dyes.
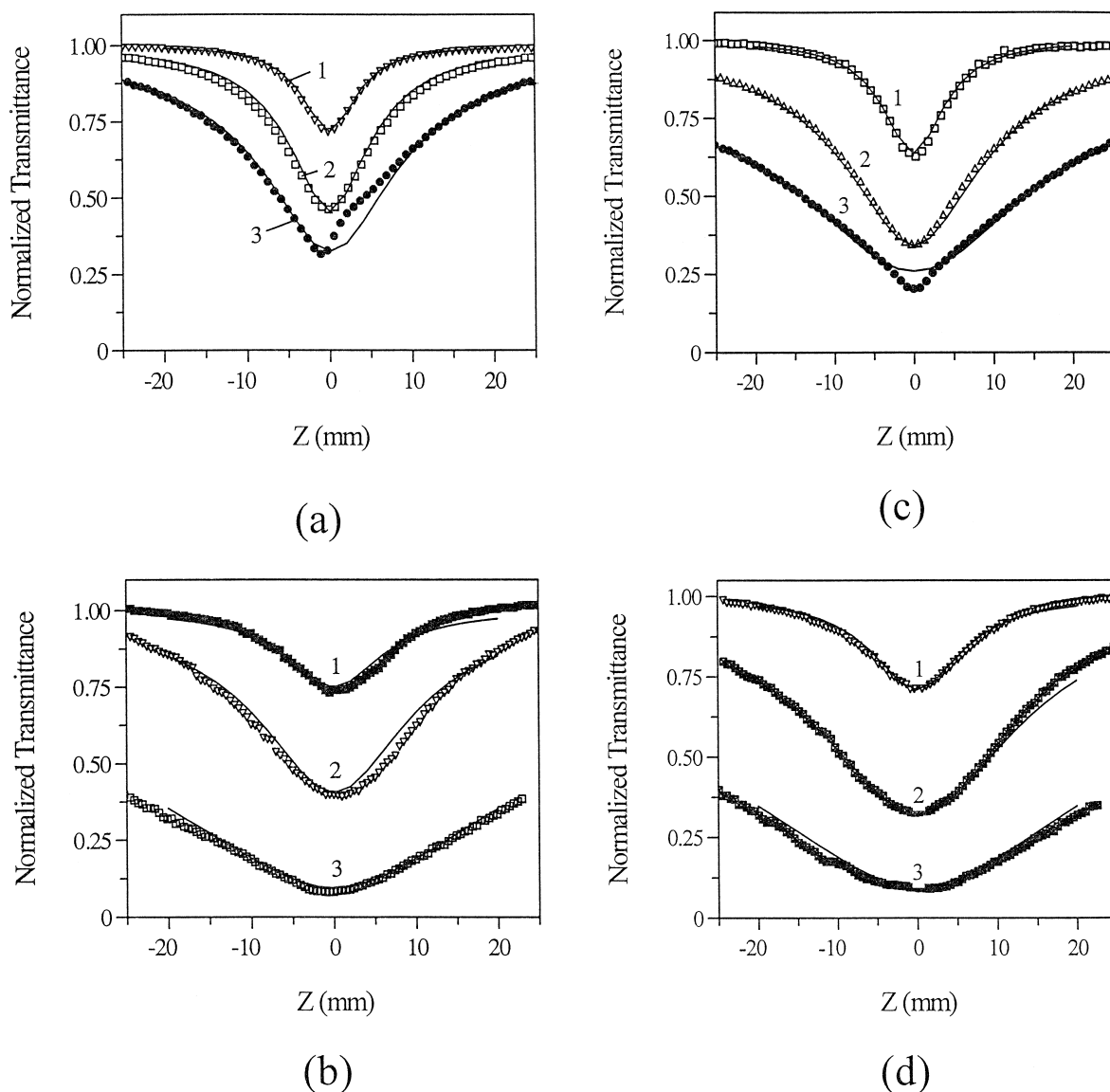
(a)

(c)

(b)

(d)

Fig. 4. Z-scan data for PD3 in (a) PUA for picosecond input; (b) PUA for nanosecond input; (c) ethanol for picosecond input; and (d) ethanol for nanosecond input. The linear transmittance is 78% and the thickness is 2 mm. The fluences in (a) are: curve 1, 0.013 J/cm^2; curve 2, 0.066 J/cm^2; and curve 3, 0.26 J/cm^2; in (b) curve 1, 0.064 J/cm^2; curve 2, 0.4 J/cm^2; and curve 3, 4.2 J/cm^2; in (c) curve 1, 0.02 J/cm^2; curve 2, 0.16 J/cm^2; and curve 3, 0.59 J/cm^2; in (d) curve 1, 0.05 J/cm^2; curve 2, 0.5 J/cm^2 and curve 3,4.2 J/cm^2. Solid lines are numerical fits using a 5-level model (see Fig. 3b) as described in Section 4. The molecular parameters used to obtain these curves are given in Table 2.

Another test of the influence of nanosecond pumping on the nonlinear properties of the dyes is to perform a Z-scan using the entire train of picosecond pulses by turning off the pulse switch-out device. However, if the interpulse spacing in the pulse train

(here 7 ns) is considerably larger than τ_{S1}, there is no accumulation of excited state population between the pulses and the train may be considered as a sequence of independent pulses. Fitting of pulse train Z-scan data shows this to be the case, so that for

these particular molecules, the pulse train yielded no additional data over single pulse data except to indicate that all relaxation processes in these molecules were effectively completed in less than 7 ns.

The main molecular parameters at 532 nm determined from the linear absorption and picosecond open aperture Z-scans are presented in Table 2. For the polymethine dyes, the largest ratios σ_{12}/σ_{01} were found for PD1, PD3, PD6 and PD8. This ratio, along with the significant linear absorption, is responsible for a very low threshold for the optical limiting response. These four dyes (PDs) have similar molecular structures but can be characterized by small differences. PD1 has an unsubstituted polymethine chromophore, while PD3, PD6, and PD8 have a phenyl-substituted 6-link-cycle polymethine chromophore.

For the two squarylium dyes, the largest cross section ratio was obtained for SD2 which combines the structure of a polymethine chromophore with the acceptor properties of the central C_4O_2-group. The poor photochemical stability of SD2 in PUA makes practical application of this dye difficult. The photostability of SD1 in PUA was much better. We also studied the spectral dependence of SD2 as discussed below.

4.1.2. Nanosecond Z-scans

In Fig. 4(b) and (d), we show open aperture Z-scans with 10 ns, 532 nm pulses for PD3 in PUA and in ethanol respectively. There are three important differences when compared with the picosecond input results. Firstly, to reach the same level of nonlinear response for nanosecond pumping, we have to significantly increase the fluence over that required for picosecond pumping (a factor greater than four, depending on the transmittance change). Secondly, saturation of the RSA is less prevalent for nanosecond pumping. Thirdly, with nanosecond pulses we do not observe photodegradation until a fluence of $\cong 6$ J/cm^2. Therefore, the decrease in transmittance is larger for nanosecond inputs. For example, the threshold for photodegradation for nanosecond inputs in PD3 in PUA was about ten times that for picosecond inputs, while the minimum transmittance for ns pulses was $\cong 6\%$ as opposed to $\cong 25\%$ for ps pulses. These same effects, although different in magnitude, were observed for all the

dyes. In addition, we find it is not possible to fit the nanosecond data with the same simple 3-level model that was used for the picosecond data. We find that to fit both the nanosecond and picosecond data, a 5-level model of the type depicted in Fig. 3(b) is required. The relatively short overall relaxation times observed (< 7 ns) suggest that the additional states are not triplets, such as are seen in phthalocyanines [22]. In addition, the triplet levels can be ignored as intersystem crossing times for polymethine dyes are about two orders of magnitude longer than τ_{S1} [2,23,24]. To investigate the nanosecond behavior more fully, we performed excite-probe measurements, described below.

4.1.3. Pump-probe measurements at 532 nm

Time-resolved excitation-probe experiments allow study of the dynamics of nonlinear absorption in dye molecules, allowing us to resolve molecular relaxation process. We performed pump-probe measurements at 532 nm on all the dyes both in PUA and in ethanol, and for probe beams polarized both parallel and perpendicular to the pumping light. The main results are presented in Figs. 5 and 6. These show the picosecond response and recovery of the probe transmittance with different polarization for PD3 and for SD1 in PUA matrices and ethanol solutions. Curves for the other samples appear qualitatively similar. As can be seen from these figures, there is a significant difference in behavior for parallel and perpendicular probe polarization. The behavior observed with the perpendicularly polarized probe showed either a flat initial response or an initial increasing loss, while the loss for parallel polarization decreased monotonically for all samples. However, analysis revealed that for both polarizations, double-exponential relaxations were observed. This behavior may be connected with rotational reorientation of the whole molecule or intramolecular configurational changes (isomerization) in the first excited state, which reduces the number of chromophores aligned in the direction of the electric field and increases the number in the perpendicular direction. Among polymethine dyes, the largest difference between parallel and perpendicular probe polarization was observed for PD1, less for PD3 and the smallest for PD6. A theory for excitation-probe measurements on materials exhibiting photoisomerization, along
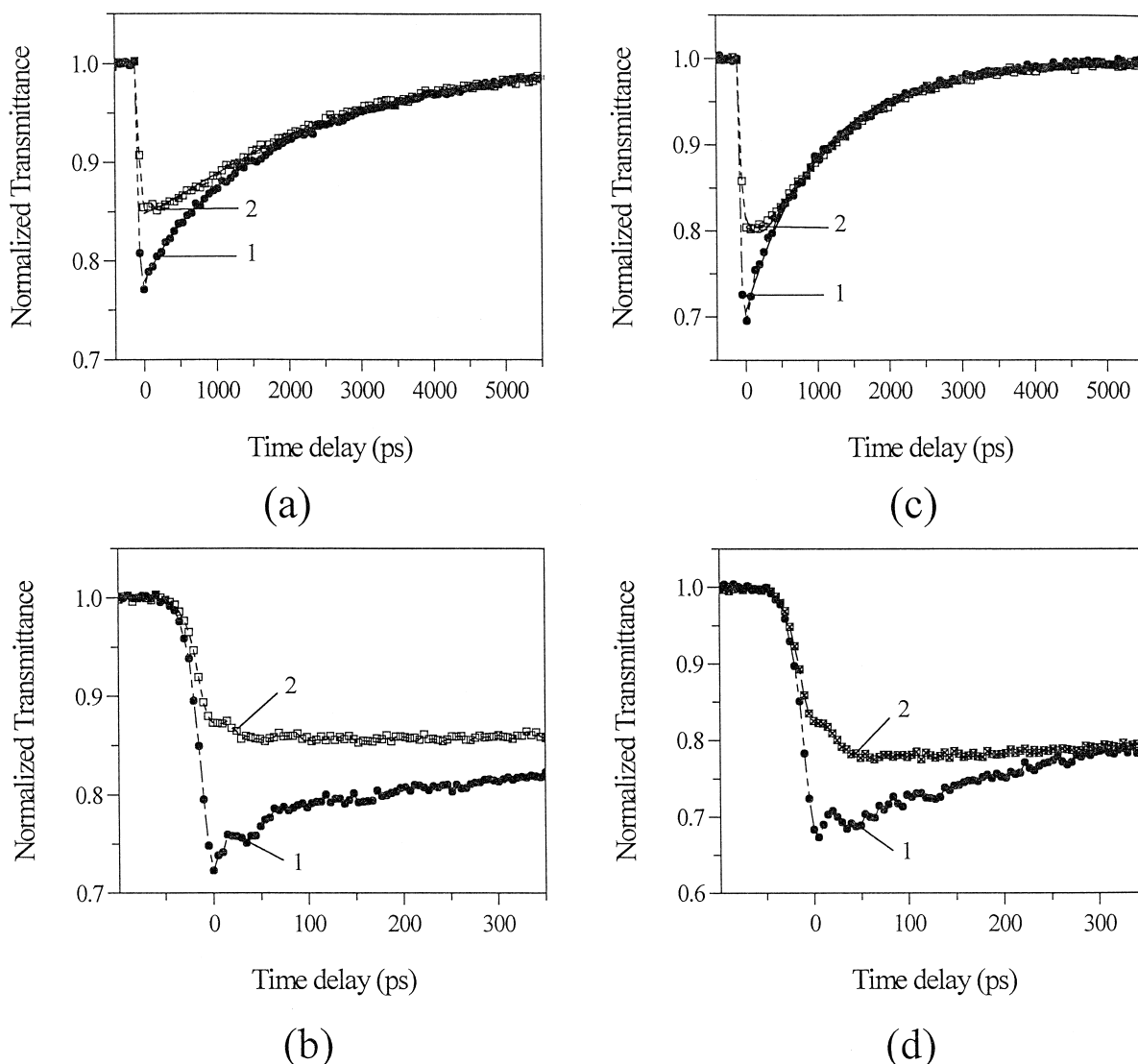
Fig. 5. Results of pump-probe experiments for PD3 in PUA, (a) and (b); and in ethanol, (c) and (d). Curves (1) correspond to a parallel polarized probe, and curves (2) correspond to a perpendicular polarized probe beam. The pump fluence is 0.0041 J/cm^2. Solid lines are numerical fits as described in Section 4.

with experimental results in the picosecond regime, is presented in Ref. [25].

The experimental data shown in Figs. 5 and 6 were fit using bi-exponential decay expressions: $T(t) = 1 - a_1 \exp(-t/\tau_S) - b_1 \exp(-t/\tau_F) + c_1$ for the parallel polarization component, and $T(t) = 1 - a_2 \exp(-t/\tau_S) - (-b_2) \exp(-t/\tau_F) + c_2$ for the perpendicular component. τ_F is the time of reorienta-

tion (described below), and τ_S is the relaxation time of the RSA. The term with the negative amplitude $(-b_2)$ reflects the formation of molecules with a changed molecular structure. This is the simplest way to empirically describe the data. From fitting pump-probe experiments we found: $\tau_F = 0.1$–0.2 ns in ethanol and $\tau_F = 0.5$–0.6 ns for PDs in PUA. For squarylium dyes, τ_F in PUA depends more on the
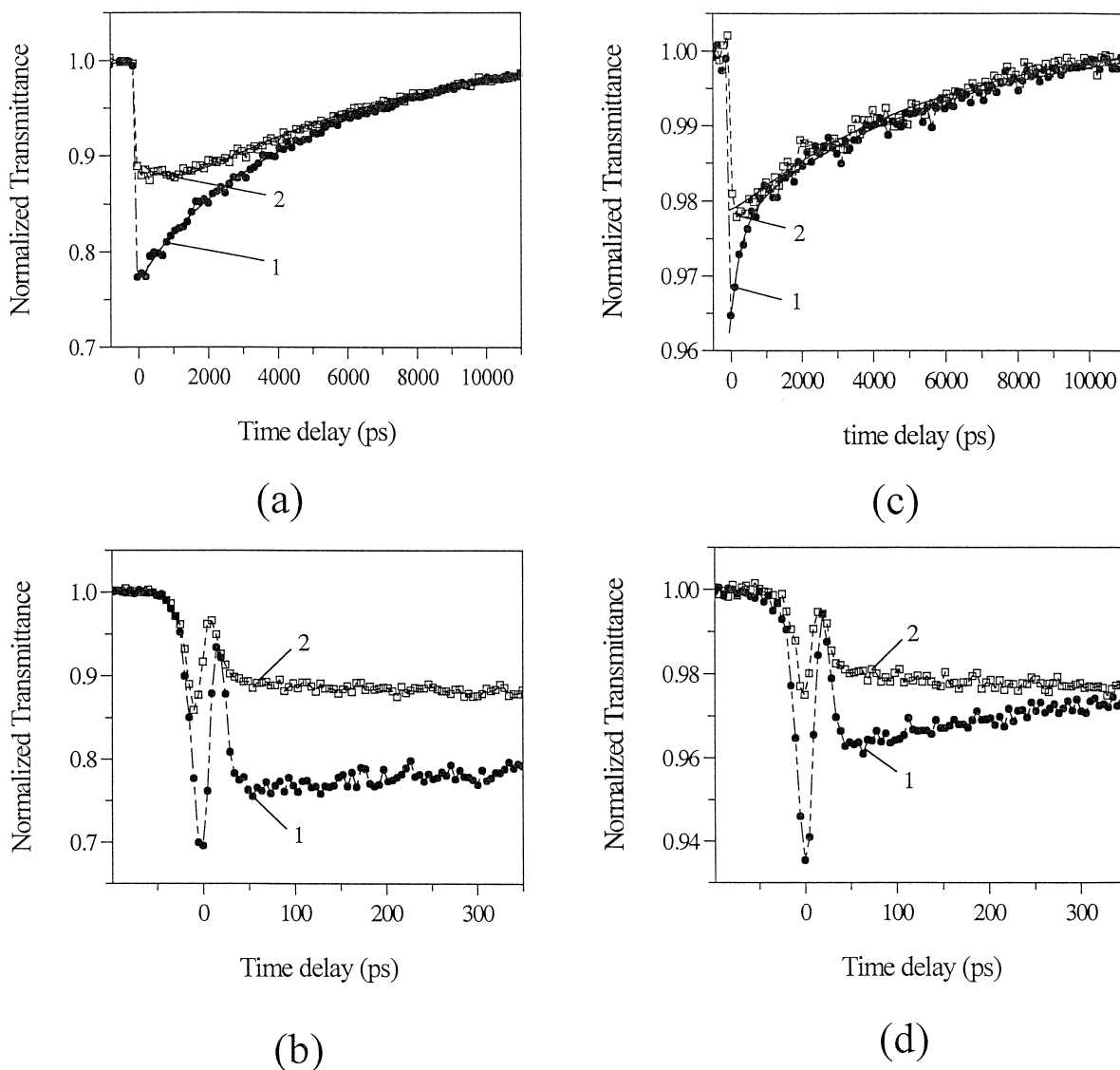
(a)

(c)

(b)

(d)

Fig. 6. Results of pump-probe experiments for SD1 in PUA, (a) and (b); and in ethanol, (c) and (d). Curves (1) correspond to a parallel polarized probe, and curves (2) correspond to a perpendicular polarized probe beam. Pumping fluence $F = 0.0045$ J/cm^2. Solid lines are numerical fits as described in Section 4.

dye structure and $\tau_F = 0.85$ ns for SD1 and $\tau_F = 2.5$ ns for SD2. In ethanol, $\tau_F = 0.3$ ns for SD1 and $\tau_F = 0.15$ ns for SD2.

Linear polarized excitation of dye molecules from S_0 to S_1 produces a light-induced anisotropy. Molecular reorientation redistributes the dipole vector of excited dye molecules, leading to a more isotropic molecular alignment. There are two channels of re-

orientations: overall rotation of the whole molecule (first channel) and formation of a new S_1^i state with a new nuclear coordinate due to intramolecular rotation of some molecular fragment (second channel). In ethanol solutions, both channels are possible. Intramolecular rotation may include a *trans–cis* isomerization process leading to a large molecular deformation such as twisting of the polymethine chain.

This twisting leads to a decrease in the effective length of the polymethine chromophore and to an increase in the effective length of the π-conjugated system in the perpendicular direction. Thus, these processes in the excited state can change the orientation of the dipole moment of the dye molecule with respect to the field. The behavior of the probe beam reflects these changes in molecular alignment. A clear example of this deformation is the large change in τ_{S1} for SD2 in ethanol and in PUA. In PUA this deformation may be a small distortion of the polymethine chain or rotation of a small rotor, e.g. a phenyl group. Based on these excite-probe data, we conclude that these conformational changes correspond to relaxation to the additional states S_1^i and S_2^i in the five-level model of Fig. 3b. Consequently, we believe these additional states are probably just the singlet states of the reconfigured molecule, i.e. iso-merization [26].

Using the excite-probe data as a starting point, we fit the nanosecond Z-scans for PD3 in both PUA and ethanol using the 5-level model. Note that τ_S in the excite-probe data does not precisely correspond to either τ_{S1} or τ_R in the 5-level model. It is a complicated function of τ_{S1}, τ_R, τ_F, and the excited-state cross sections. These fits correspond to the solid lines in Fig. 4(b) and (d). The molecular parameters determined from these fits are shown in Table 3. Consistent with the pulse train data, fitted relaxation times τ_F and τ_R are less than the pulse train inter-pulse spacing.

The lifetimes determined from pump-probe measurements are summarized in Table 2. For polymethine dyes in PUA, the longest lifetimes $\tau_{S1} = 2.1–2.5$ ns were related to unsubstituted PD1, and phenyl-substituted PD3 as well as PD8 having 6-link-cycles in the polymethine chain. For the dye PD6 with the more complicated π-electron system in the end chromophore groups and the same structure of the polymethine chromophore, there was a de-crease in τ_{S1} to $\cong 1$ ns (e.g. compare PD3 and PD6). The same trend with change in chemical structure can be seen in the series of dyes with 5-link-cycles in the polymethine chain. For PD2, PD5 and PD7, the lifetimes are in the range of 1.4–1.7 ns, with a decrease to 0.8 ns for PD10. The lifetimes in PUA were typically twice as long as in ethanol solutions, which we attribute to a restriction of molecular motion in the polymeric host. Among the PDs, PD3 has the largest ratio and was singled out for more intensive studies including measuring its spectral dependence with the OPO as discussed below.

Interesting results were obtained for squarylium dyes on short timescales. For temporally overlapped pulses in the squarylium dyes, strong beam-coupling effects are seen, with the sign of energy transfer between pump and probe changing as a function of delay. This can be ascribed to stimulated Rayleigh-wing scattering (SRWS) resulting from molecular reorientation and/or conformational changes along with slightly chirped laser pulses, as previously described in Ref. [27]. While these coherent coupling effects (two-beam coupling) are also observed for the PDs, the magnitude of the effect is much reduced. The difference between ethanol and PUA hosts can be seen only on these short time scales (see Fig. 6(b),(d)), where the PUA shows a much reduced beam coupling effect, as would be expected due to the restriction of molecular motion imposed by the host. These coherent coupling effects are not important for the studies of RSA reported here.

On longer time scales, SD1 is characterized by the largest value of $\tau_{S1} \cong 6$ ns, and this value is nearly host independent. According to Ref. [12], this result can be explained by the formation of hydrogen bonds between oxygen atoms in the central ring and electron-donor hydroxyl groups leading to a more rigid structure. For SD2, $\tau_{S1} = 5$ ns in PUA and only 0.4 ns in ethanol. This drastic difference in lifetimes is probably connected with the internal twisting around the C–C linkages between the central C_4O_2 group and electron-donor end fragments in ethanol solution.

4.1.4. Optical limiting experiments at 532 nm

The nanosecond optical limiting responses at 532 nm of PD1 in PUA, PD3 in ethanol and in PUA, are

Table 3
Molecular parameters of PD3 for a five-level model

	σ_{12}^i ($\times 10^{-16}$ cm^2)	τ_F (ns)	τ_R (ns)	τ_{S2} (ps)
PD3 in PUA	1	0.5	2	3
PD3 in ethanol	5	0.2	0.8	3

presented in Fig. 7(a). All the samples had a linear transmittance between 69 and 78%. The largest changes in transmittance were obtained for PD3. As can be seen from the limiting curves at high inputs in Fig. 7(a), the transmittance change with increasing input decreased so that the limiting effectiveness was reduced (i.e. the curve became nearly flat). This apparent 'saturation' of the nonlinear behavior can be modeled using the 5-level model and the saturation is less for nanosecond pulses than for picosecond pulses, as discussed above. Below about 6
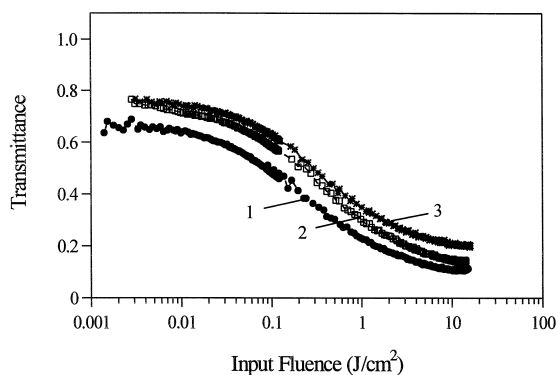
(a)
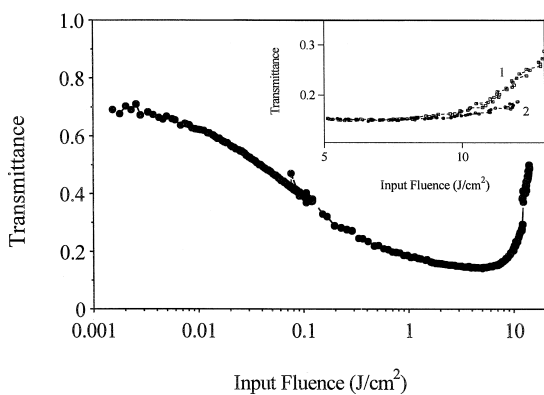
(b)

Fig. 7. (a) Optical limiting curves: curve 1, for PD1 in PUA with linear transmittance 69%, and thickness 2 mm; curve 2, for PD3 in PUA and curve 3, for PD3 in ethanol, with linear transmittance 78% and thickness 2 mm for both polymeric and liquid samples; (b) limiting curves for SD2 in PUA (linear polarization) with linear transmittance 70% and thickness 0.72 mm. Insert shows photochemical bleaching of the dye for (1) linear polarization and for (2) circular polarization.

J/cm^2, the changes in transmittance shown in Fig. 7(a) are reversible. However, at even higher inputs photochemical decomposition of the dye can be observed. This occurs for SD2 at lower fluences, where an irreversible increase in transmittance is observed at input fluences $> 3 \; J/cm^2$, as shown in Fig. 7(b).

We measured limiting curves for PD3 and SD2 in PUA at 532 nm for both linear and circular polarization. For PD3 in PUA no difference in optical limiting response was observed even above levels where photodegradation occurs. The same behavior was found for SD2 for fluences below $\cong 3 \; J/cm^2$. Above this level in SD2, photodegradation is more rapid for linear than for circular polarization at the same fluence which is probably connected with the larger excited-state population in case of circular polarization, as shown in the inset of Fig. 7(b). The use of circular polarization could help extend the operational lifetime of optical limiting elements based on SD2. This could be accomplished by placing a quarter-wave plate at the input to the limiting device.

5. Wavelength dependence studies with an optical parametric oscillator

5.1. Optical parametric oscillator Z-scan experiments

For applications such as optical limiting, it is important to determine the dependence of the nonlinear optical parameters over a broad spectral range. Here, we report the results of Z-scan measurements of two of these dyes at wavelengths from 440 to 650 nm measured with the picosecond OPO. We measure the polymethine and squarylium dyes in PUA that show the best RSA behavior in the 532 nm wavelength studies, namely PD3 and SD2. Ground-state cross sections determined from the linear spectrum are shown in Fig. 8, while values for σ_{12}/σ_{01} based on a 3-level model, determined from the Z-scan measurements, are shown in Fig. 9. The polymethine dye PD3 showed RSA over a broad spectral range for wavelengths shorter than $\cong 620$ nm, (from $\cong 480$ to $\cong 620$ nm) while SD2 showed RSA over a relatively narrow range from $\cong 500$ nm to 560 nm.
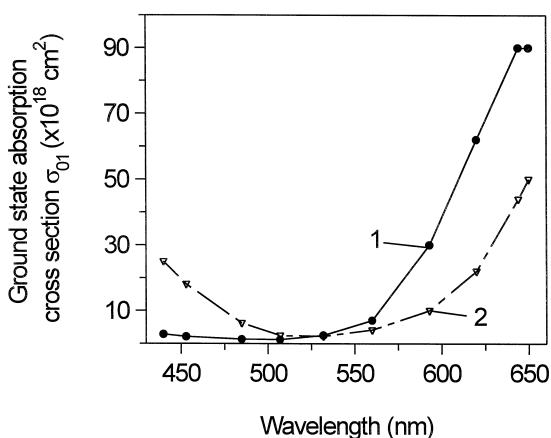
Fig. 8. Spectra of ground state absorption cross sections for (1) SD2 and (2) PD3 in PUA as calculated from linear transmittance spectrum, concentration and sample thickness. All the cross sections are larger than 1×10^{-18} cm^2.

Values of $\sigma_{12}/\sigma_{01} < 1$ correspond to saturable absorption, which occurs at wavelengths where the linear absorption becomes appreciable.

5.2. Optical parametric oscillator pump-probe measurements

Fig. 10 shows an example of pump-probe data taken with the picosecond OPO on PD3 in PUA (using perpendicular polarized beams). From these measurements with the absolute irradiance deter-
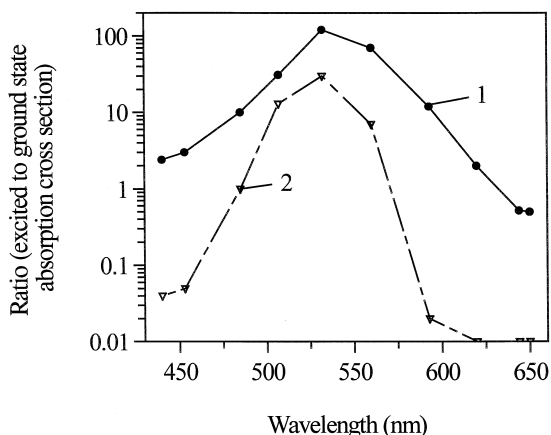

Fig. 9. Spectral dependence of the ratio of excited to ground state absorption cross section for (1) PD3 and (2) SD2 in PUA. For ratios, σ_{12}/σ_{01} larger than unity the samples show RSA.
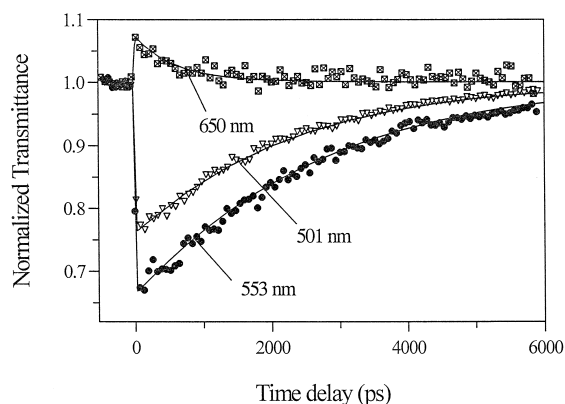

Fig. 10. Experimental pump-probe results for PD3 in PUA using the picosecond OPO tuned to 501, 553, and 650 nm. Dotted lines are experimental data and solid lines fitting curves: RSA ($\sigma_{12}/\sigma_{01} = 54$), $\tau_S = 2.1$ ns at 501 nm, 0.01 J/cm^2; RSA ($\sigma_{12}/\sigma_{01} = 65$), $\tau_S = 2.3$ ns at 553 nm, 0.0086 J/cm^2; and SA ($\sigma_{12}/\sigma_{01} = 0.5$), $\tau_S = 0.6$ ns at 650 nm, 0.0086 J/cm^2.

mined from a combination of pulse width and spot size measurements, the absolute value of the excited state absorption cross section can be determined from the initial value of the induced loss (i.e. at zero time delay). These values agree within experimental errors of $\cong \pm 20\%$ with the values obtained from the open aperture Z-scans. The saturable absorption at 650 nm exhibited a shorter relaxation time than the RSA at other wavelengths as calculated in this 3-level model. If the excited level is assumed to be the same for all the frequencies measured, the lifetime of S_1 should not depend on wavelength. The use of the 5-level model readily allows the lifetime to be independent of wavelength as expected. In fact, allowing level lifetimes to vary independently to obtain a best fit gives ranges of values for lifetimes that are consistent with a constant lifetime of S_1. The variable decay times observed in experiments are due to the relative wavelength dependencies for the two separate singlet excited states, e.g. as S_1 decays to S_1^i the absorption could decrease or increase depending on the relative cross sections.

6. Conclusions

We characterized the nonlinear optical properties of a series of polymethine and squarylium dyes in

two host media: liquid ethanol and the elastopolymer polyurethane acrylate (PUA). We were able to systematically modify the photophysical properties of the dyes, in particular, the frequency difference between the absorption resonance and the pumping laser frequency (532 nm), through changes in molecular structure. We determined absorption cross sections and in particular the ratio of the excited-state to ground-state absorption cross sections and found ratios in excess of 100 for some polymethine dyes at 532 nm (PD1, PD3, PD6 and PD8). These ratios are the largest measured to our knowledge while keeping a large ground state absorption cross section ($>$ 10^{-18} cm^2). The dyes exhibiting these large ratios have similar molecular structures. The parameters of these molecules for nonlinear applications such as optical limiting show a significant improvement over the first set of this class of dyes studied [2] and indicate that further improvement of the photophysical parameters may be possible. We also determined the nonlinear properties of two squarylium dyes SD1 and SD2, characterized by quite different molecular structures. The distinguishing feature of these dyes is a lower cross section ratio but a comparatively longer excited state lifetime, τ_{S1} (6 ns for SD1 in both ethanol and PUA, and 5 ns for SD2 in PUA). The best nonlinear response was found for SD2, which combines the structure of a polymethine chromophore with the acceptor properties of the central C_4O_2-group. Also, the bandwidth of RSA is reduced with respect to the PDs and the photochemical stability of SD2 in PUA is rather low. The photostability of SD1 in PUA is much better. Therefore, there is some hope that this property can be improved.

While the large cross section ratios are favorable for application to optical limiting, large changes in transmittance could not be obtained for picosecond pulses. This reduction of the limiting effectiveness at higher inputs can be explained by saturation of the S_1 to S_2 transition due to the short but finite lifetime of the S_2 level (see Section 4.1.1). This is explained more fully in Refs. [18,21]. The values of τ_{S2} for the dyes studied here are presented in Table 2. The relative uncertainties are large due to the limited range of inputs between where the saturation could be observed and where bleaching began. From these studies we found that $\tau_{S2} \approx 0.2–3$ ps in ethanol and $1–3$ ps in PUA depending on the dye structure. The

smallest values of τ_{S2} in ethanol were found for PD1, PD10 and SD1, and in PUA for PD4, PD10 and SD1. For PD2, PD6 and SD2, the τ_{S2}'s are almost equal in the two hosts. The largest values of $\tau_{S2} \approx 3$ ps were found for PD1, PD3, PD8 and SD2 in PUA. For the dyes PD4, PD6 and SD2 in PUA, τ_{S2} is so short that the minimum transmittance is only weakly influenced. In this case, the major factors determining the transmittance for picosecond pulses are the photochemical decomposition of dye molecules and the damage threshold of the polymeric medium. Limiting of nanosecond pulses is affected much less by this saturation, as τ_{S2} is much shorter than the pulsewidth. Explanation of the nanosecond data requires a 5-level model as explained below.

While the 3-level model adequately explains our picosecond data, it cannot consistently explain the nanosecond data either for Z-scan or for pump-probe measurements. We therefore proposed a five-level model consisting of all singlet states, which includes reorientational processes in the first excited state, see Fig. 3(b). The nature of these processes may be twofold: overall rotation of the whole molecule or intramolecular configurational changes. For ethanol solutions at room temperature, polarization kinetics may include both processes. In polymeric media the overall rotation of dye molecules does not contribute on the time scale observed in our experiments. Therefore, we consider conformational changes, i.e. isomerization, as an important part of the excited-state dynamics.

The results of pico-and nanosecond Z-scans and excitation-probe experiments may be explained by a five-level model (all singlet states), which includes $S_0 \to S_1 \to S_2$ absorption, conformational changes in the S_1 state leading to the formation of a new singlet S_1^i state with a new molecular configuration, $S_1^i \to S_2^i$ reabsorption and restoration of the primary homogeneous distribution in the ground state S_0. This model was used to accurately model the response of PD3 for all experiments performed. Using the five-level model, which includes $S_0 \to S_1 \to S_2$ and $S_1^i \to S_2^i$ absorption as well as reorientational processes in S_1, we could obtain fits for both pico- and nanosecond inputs with the same molecular parameters. Examples of numerical fits are shown in Fig. 4 for pico- and nanosecond Z-scans.

Pump-probe polarization studies of the dynamics of the excited-state absorption reveal a large difference in the behavior of the probe beam with parallel and perpendicular orientation to the polarization of the excitation beam. While the parallel probe beam shows a fast decay of nonlinear transmittance, the perpendicular probe beam at the same time shows either an increase or constant value of nonlinear response. This behavior is explained by the conformational changes in the first excited state, which reduce the number of chromophores aligned in the direction of the electric field and increase the number in the perpendicular direction. These processes could include overall rotation of dye molecules in ethanol and intramolecular configuration changes in both ethanol and PUA. Excited-state relaxation dynamics of polymethine dyes have been an area of intense research in recent years [28–32]. It is well-known [33] that *trans–cis* isomerization in the excited states of polymethine dyes in low viscosity solutions produces one of the most important nonradiative decay pathways. The quantum yield for isomerization strongly depends on the molecular structure of the dye, temperature and solvent viscosity. In polymeric media *trans–cis* conformational changes may be more restricted due to rigidity of the media. Relaxation processes within the excited state of dye molecules in polymeric media are less well investigated. Our current studies and previous observations [11] allow us to conclude that in elastic PUA the small conformational changes of PD's, such as rotations of phenyl groups either in the polymethine chromophore or in the end groups, are possible. These rotations are almost barrierless and may be more closely related to free volume effects than to macroscopic viscosity [34,35].

Thus, our understanding is that the main factor reducing the effectiveness of optical limiting in the nanosecond regime is the relatively short lifetime of the first excited state S_1, which is reduced by intramolecular conformational processes. Therefore, despite the large ratio of σ_{12}/σ_{01} found for some polymethine dyes (the largest among organic dyes), this advantage cannot be fully realized at present for optical limiting. Molecular engineering methods to inhibit the *trans–cis* changes are under investigation. We expect that further research on PDs and SDs may produce new dyes with increased excited-state lifetimes, reduced upper-state saturation and improved photochemical stability.

Acknowledgements

References

[1] K. Mansour, P. Fuqua, S.R. Marder, B. Dunn, J.W. Perry, Proc. SPIE 2143 (1994) 239.

[2] O.V. Przhonska, J.H. Lim, D.J. Hagan, E.W. Van Stryland, M.V. Bondar, Y.L. Slominsky, J. Opt. Soc. Am. B 15 (1998) 802.

[3] P.A. Miles, Bottleneck optical limiters: the optimal use of excited-state absorbers, Appl. Opt. 33 (1994) 6965–6979.

[4] J.W. Perry, K. Mansour, I.-Y.S. Lee, X.-L. Wu, P.V. Bedworth, C.-T. Chen, D. Ng, S.R. Marder, P. Miles, T. Wada, M. Tian, H. Sasabe, Science 273 (1996) 1533–1536.

[5] J.W. Perry, Organic and metal-containing reverse saturable absorbers for optical limiters, in: H.S. Nalwa, S. Miyata (Eds.), Nonlinear Optics of Organic Molecules and Polymers, CRC Press, New York, 1997, pp. 813–840 (Chapter 13).

[6] E.W. Van Stryland, D.J. Hagan, T. Xia, A.A. Said, Application of nonlinear optics to passive optical limiting, in: H.S. Nalwa, S. Miyata (Eds.), Nonlinear Optics of Organic Molecules and Polymers, CRC Press, New York, 1997, pp. 841–860 (Chapter 14).

[7] A.A. Said, T. Xia, D.J. Hagan, A. Wajsgrus, S. Yang, D. Kovsh, M.A. Decker, S. Khodja, E.W. Van Stryland, Proc. SPIE 2853 (1996) 18.

[8] D.J. Hagan, T. Xia, A.A. Said, T.H. Wei, E.W. Van Stryland, Int. J. Nonlin. Opt. Phys. 2 (1993) 483–501.

[9] T.H. Wei, D.J. Hagan, M.J. Sence, E.W. Van Stryland, J.W. Perry, D.R. Coulter, Appl. Phys. B 54 (1992) 46.

[10] D.R. Coulter, V.M. Miskowski, J.W. Perry, T.-H. Wei, E.W. Van Stryland, D.J. Hagan, Proc. SPIE 1105 (1989) 42–51.

[11] O.V. Przhonska, M.V. Bondar, J. Gallay, M. Vincent, Yu. Slominsky, A.D. Kachkovski, A.P. Demchenko, Photophysics of dimethylamino-substituted polymethine dye in polymeric media, to be published.

[12] G.W. Scott, K. Tran, J. Phys. Chem. 98 (1994) 11563–11569.

[13] M. Samoc, A. Samoc, B. Luther-Davies, M. Woodruff, Pure Appl. Opt. 5 (1996) 681–687.

[14] V.I. Bezrodnyi, M.V. Bondar, G.Y. Kozak, O.V. Przhonska, Y.A. Tikhonov, J. Appl. Spectrosc. 50 (1989) 441–454.

[15] M. Sheik-bahae, A.A. Said, T.H. Wei, D.J. Hagan, E.W. Van Stryland, Journal Quantum Electronics 26 (1989) 760–769.

[16] Materials for optical limiting, in: R. Crane, K. Lewis, E. Van

Stryland, M. Khoshnevisan (Eds.), Materials Research Society, vol. 374, 1994.

[17] E.P. Ippen, C.V. Shank, Ultrashort light pulses, in: S.L. Shapiro (Ed.), Topics in Applied Physics, vol. 18, Springer-Verlag, Berlin, 1977, pp. 83–122.

[18] T.-H. Wei, T.-H. Huang, H.-D. Lin, S.-H. Lin, Appl. Phys. Lett. 67 (1995) 2266–2268.

[19] S. Hughes, G. Spruce, B.S. Wherrett, K.R. Welford, A.D. Lloyd, Opt. Commun. 100 (1993) 113–117.

[20] S.N.R. Swatton, K.R. Welford, S.J. Till, J.R. Sambles, Appl. Phys. Lett. 66 (1995) 1868–1870.

[21] T.-H. Wei, Ph.D. dissertation, Univ. of North Texas, 1992.

[22] J.-P. Fouassier, D.-J. Lougnot, J. Faure, Chem. Phys. Lett. 35 (1975) 189–194.

[23] X.R. Zhu, J.M. Harris, Chem. Phys. 142 (1990) 301–309.

[24] D. Fassler, K.-H. Feller, J. Mol. Struct. 173 (1988) 377–387.

[25] S. Rentsch, B. Wilhelmi, J. Mol. Struct. 114 (1984) 1.

[26] K.-H. Feller, R. Gadonas, V. Krasauskas, Laser Chem. 8 (1988) 39–47.

[27] A. Dogariu, T. Xia, D.J. Hagan, A.A. Said, E.W. Van Stryland, N. Bloembergen, J. Opt. Soc. Am. B 14 (1997) 796.

[28] M.R.V. Sahyun, N. Serpone, J. Phys. Chem. A 101 (1997) 9877–9883.

[29] R.W. Redmond, I.E. Kochevar, M. Krieg, G. Smith, W.G. McGimpsey, J. Phys. Chem. A 101 (1997) 2773–2777.

[30] J. Rodriguez, D. Scherlis, D. Estrin, P.F. Aramendia, R.M. Negri, J. Phys. Chem. A 101 (1997) 6998–7006.

[31] E.N. Kaliteevskaya, T.K. Razumova, G.M. Rubanova, Opt. Spectrosc. (USSR) 60 (1986) 166–168.

[32] I. Martini, G.V. Hartland, Chem. Phys. Lett. 258 (1996) 180–186.

[33] R.E. Di Paolo, L.B. Scaffardi, R. Duchowicz, G.M. Bilmes, J. Phys. Chem. 99 (1995) 13796–13799.

[34] J.F. Rabek, Photodegradation of Polymers, Springer-Verlag, Berlin, 1996, pp. 98–108.

[35] J.L. Duda, J.M. Zielinski, in: P. Neogi (Ed.), Diffusion in polymers, Marcel Dekker, 1996, pp. 143–171.